Techniques and Modes for Multi-Channel SAR Instruments

Marwan Younis, Felipe Queiroz de Almeida, Paco López-Dekker, and Gerhard Krieger
German Aerospace Center (DLR), Oberpfaffenhofen, Germany

Abstract

SAR instruments with multiple transmit/receive channels allow for a variety of operation modes. The trade-space includes the instrument and antenna parameters designed to enable various techniques (operation modes). These are utilized to achieve a required SAR performance derived from the mission and user requirements. Finding a solution in this multi-dimensional trade space of inter-dependent parameters is not trivial and often involves the compromise of parameters. This paper addresses the topic of SAR instrument design tailored to a set of operation modes. It explains the SAR techniques and reports the performance highlighting possible compromises between techniques and system efficiency.

1 Introduction

Single-channel SAR sensors operate within a trade-space subject to the "fundamental limitation" limiting simultaneous wide swath coverage and high azimuth resolution. Utilizing full polarimetry or interferometry typically results in further performance degradation. Currently, there is a clear trend towards multi-digital-channel systems; examples are TerraSAR-X (two channels as a by-product of the redundancy concept), RADARSAT-2 for ATI applications, ALOS-2 to increase the azimuth resolution. This step towards multi-channel SAR instruments marks a paradigm change as a consequence of research activity results in the last decade. The main innovative characteristic of forthcoming generations of SAR systems is the use of multiple elevation and/or azimuth receiver channels combined with digital beamforming (DBF) capability [1, 2, 3]. This allows for the synthesis of multiple or dynamic digital receiver beams. Further, multiple transmit channels are being suggested as an extension to DBF systems.

The virtue of Multi-Channel SAR is that it extends the dimensionality of the trade-space. This allows the conception of new systems which overcome the "fundamental limitation" of conventional SAR. A good example is the simultaneous High-azimuth-Resolution and Wide-Swath SAR also known as HRWS [4], which improves two performance parameters without sacrificing others [5, 6]. It is comprehensible that multi-channel SAR allow new system architectures and novel combinations of operation techniques (modes).

It is the aim of this paper to introduce the trade-space of multi-channel SAR and show implementable instrument designs. The approach is to introduce a set of parameters describing the system and the performance and show how they can be traded by virtue of system examples. The instrument description remains at a conceptual level to avoid irrelevant technical details.

2 System Requirements and Trade-Space Parameters

The most relevant system and performance parameters for the L-band SAR considered in this paper are shown in **Figure 1**. Here the system parameters basically describe the instrument both in terms of quantities fixed by the system design such as antenna dimensions, and parameters which can be altered during operation (e.g. the Pulse Repetition Frequency: PRF).

The system parameters will be altered for the various implementations considered later, however, to allow for a "fair" comparison (and to limit the trade space dimension), three system parameters will be fixed. As shown in **Figure 1** these are the center frequency, total average Tx power, and orbit height (resulting, for the chosen swath width of 400 km in an incidence angle range from $25°$ to $45°$).

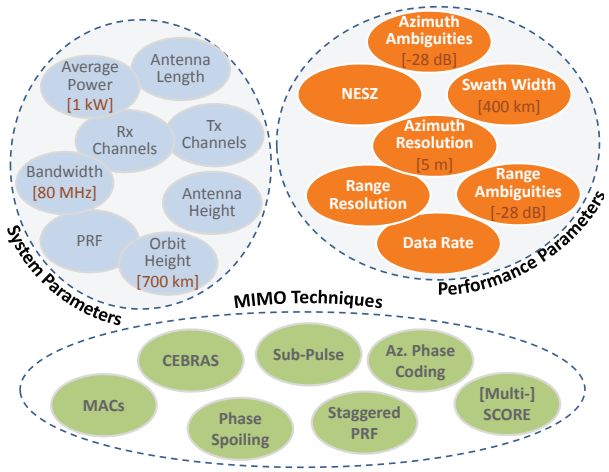

Figure 1: Relevant system and performance parameters for SAR. These parameters can be optimized using different MIMO techniques (modes).

The performance parameters are used to describe how good the system actually is. The limiting values of a sub-set of the performance parameters are usually derived from the mission requirement, as is the case for the ambiguity level. Others may simply be a result of the system parameters, such as the range resolution assuming, here, that the chirp bandwidth is fixed. The actual values of the performance parameters result from a model- or simulation-based system analysis and obviously depend on the system parameters. To achieve the desired performance, various "MIMO" techniques might be used. Thus, for example the data rate (performance) depends on the system (chirp bandwidth) but also shows how efficiently the system is operated (techniques).

The emphasis of this paper is on the various SAR techniques, depicted in **Figure 1**, that can be utilized for multi-channel instruments to yield a desired performance. To demonstrate this, we first aim at determining the antenna size of a single-channel SAR that fulfils the swath and resolution performance when operated in stripmap mode. **Figure 2a** illustrates the interaction between system and performance parameters. A system that achieves an azimuth resolution of $5\,\mathrm{m}$ has, e.g., only a swath width of less than $140\,\mathrm{km}$. Similarly, trying to increase the swath width leads to a worsening of the azimuth resolution. The reason can basically be traced back to Shannon's sampling theorem. This shows that the requirement simply cannot be met with a conventional SAR in stripmap mode.

(a) conventional single-channel SAR

(b) multi-azimuth receive channel SAR

Figure 2: Improving the azimuth resolution causes different parameters interactions depending on the system.

3 SAR System Options

In this section various SAR instrument and antenna options are investigated. The presented system designs should be understood as conceptional in the sense that further optimization would improve performance by several dBs. However, here the intention is to show how the various techniques can be utilized and to report on their system efficiency, which is a measure understood here as an indication of how efficiently the system resources are used to achieve the required performance.

[1] up to a size where the pulse extension loss becomes relevant [7]

3.1 Single Swath Stripmap Mode

A straightforward approach to reach the required swath width and azimuth resolution is shown in **Figure 2b** and consists of dimensioning the Rx antenna so as to yield the swath width while utilizing Multiple Azimuth Channels (MACs) to reach the azimuth resolution. By this the resolution is decoupled from the total antenna length. The system parameters are obtained by determining the PRF which allows imaging a $W_{sw} = 400\,\mathrm{km}$ swath. This gives $430\,\mathrm{Hz}$ when using the approximation

$$PRF \leq \frac{c_0}{2W_{sw}\sin\eta_i} \tag{1}$$

where η_i is the incidence angle and c_0 the velocity of light. The total antenna length is determined according to the condition of uniform azimuth sampling [2]

$$L_{Rx}^{\text{unif}} = \frac{2v_{sat}}{PRF} \tag{2}$$

which yields a considerable value of $L_{Rx} = 34\,\mathrm{m}$! Knowing that the individual azimuth element must cover a Doppler bandwidth corresponding to the azimuth resolution (or just applying the known approximation for the azimuth resolution $\delta_{az} = L_{Rx}/2N$) leads to a number $N = 4$ of azimuth channels.

The dimensions of the Tx antenna are set so as to illuminate the whole swath in elevation and the necessary Doppler bandwidth $B_D = v_{sat}/\delta_{az}$ in azimuth. The resulting Tx antenna of $12\,\mathrm{m} \times 0.8\,\mathrm{m}$ is relatively small, so to compensate its low gain the Rx antenna height can be increased[1] if the SCan-On-REceive (SCORE) [5, 6] technique is used, which requires multiple elevation channels. The performance parameters of the system are quite good as shown in **Figure 3**. The azimuth ambiguity level is constant at $-26\,\mathrm{dB}$. The NESZ follows the shape of the wide transmit pattern [8].

However, such a system can practically not be realized due to the tremendous antenna length.

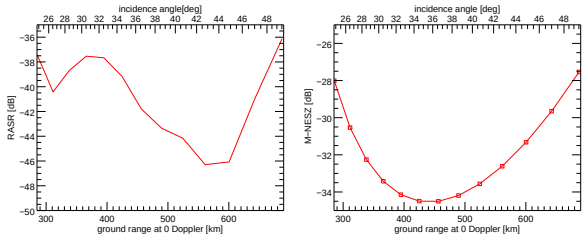

(a) RASR **(b)** NESZ

Figure 3: Performance of single swath stripmap system showing the range-ambiguity-to-signal ratio (RASR) and noise-equivalent sigma-zero (NESZ) vs. ground range.

3.2 Single Swath Sub-Pulse Mode

A possibility to reduce the antenna length of the previous system to approximately half is to use sub-pulse techniques [9]. The basic idea is to illuminate the wide swath

by two sub-pulses from two different azimuth positions by using two Tx antennas. Adding the second Tx antenna [10, 11] allows the system to be operated such that two pulses are transmitted within each Pulse Repetition Interval (PRI) where typically each sub-pulse is delayed by a small fraction of the PRI with respect to previous one as shown in **Figure 4**.

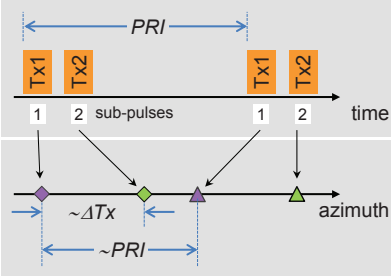

Figure 4: Two sub-pulses showing that the position of the spatial samples depends on the Tx antenna separation and the PRI.

Doubling the number of Tx pulses within the same time interval consumes twice the power [9], but the number of received samples per PRI (i.e. the spatial sampling) is doubled which, here, allows reducing the Rx antenna length to half the values given by (2), i.e. $L_{Rx} = L_{Rx}^{\text{unif}}/2 = 17.4\,\text{m}$. The spatial distance between the azimuth samples of the two sup-pulses is mainly determined by phase center separation of the Tx antennas. Uniform sampling is achieved when $\Delta_{Tx} = L_{Rx}/2$, which, for a single Tx/Rx antenna aperture, requires that the length of each Tx antenna be $L_{Tx} = L_{Rx}/2 = 8.7\,\text{m}$. The echo signals of the two sub-pulses arrive at nearly the same time at the receiver. To separate the two echoes multi-SCORE is utilized here, where two receive beams are generated, each one maximized to the direction of arrival of one sub-pulse while suppressing the energy of the other [10, 11]. The Rx antenna height H_{Rx} required to place a pattern null at the interfering sup-pulse is computed according to [3]:

$$H_{Rx} = \frac{2\lambda r \tan\eta_i}{c_0 \Delta\tau} \tag{3}$$

where r is the slant range and $\Delta\tau$ is the time delay between the the start of the two sub-pulses, respectively. Taking a single sub-pulse duty cycle of 6 % gives $H_{Rx} = 13.4\,\text{m}$ necessary to suppress the pulses at far range (worst case).

The SAR performance is shown in **Figure 5** in terms of the NESZ and Doppler pattern. The azimuth performance is comparable to the previous single-swath stripmap system, although here a total of 3 azimuth channels are used (this effectively increases the azimuth sampling since it corresponds to 6 samples per PRI, whereas the previous system had 4 samples per PRI) to compensate for the shorter Tx antenna length.

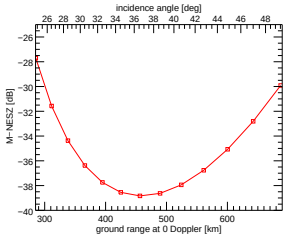

(a) NESZ

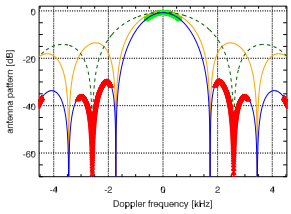

(b) Azimuth Pattern

Figure 5: Noise-equivalent sigma-zero versus ground range and azimuth pattern for single swath stripmap system utilizing sub-pulses.

Note that the SAR system described here is truly a MIMO SAR utilizing both multiple-transmit and multiple-receive channels.

3.3 Multi-Azimuth ScanSAR

Alternatively the ScanSAR burst mode may be used to cover the wide swath while utilizing multiple azimuth channels (MACs) for the required azimuth resolution [12], as has been suggested within the Sentinel-1 follow-on Study [13]. A straightforward approach would adopt the C-band system parameters, which remain the same in azimuth due to the beamwidth to Doppler frequency scaling, while the antenna height would need to be increased by a factor of 4.3 (C-band to L-band center frequency ratio). Here, an alternative design is presented which results in an Rx antenna dimension of $12.2\,\text{m} \times 2.8\,\text{m}$ and 8 azimuth channels. As shown in the timing diagram of **Figure 6a** the system is operated in $n_{burst} = 4$ bursts, which is the minimum number needed if nadir echoes are taken into account by the timing considerations[2].

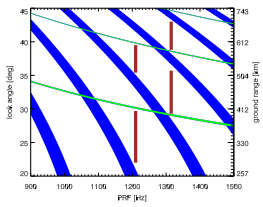

(a) Timing Diagram

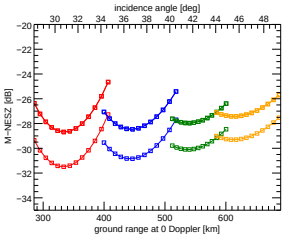

(b) NESZ

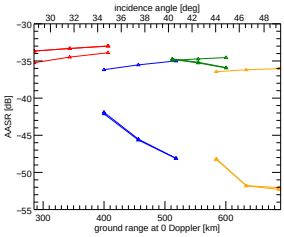

(c) AASR

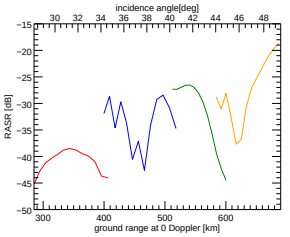

(d) RASR

Figure 6: Timing diagram and SAR performance of the 4-burst ScanSAR MACs system.

[2] An alternative 3 burst operation would result in a somehow similar antenna size but require only 6 azimuth channels. This is at the expense of having to suppress the nadir echo through elevation beam-forming techniques.

Figure 6b shows that the NESZ variation within the swath is smaller compared to the previous modes, which is a result of the reduced sub-swath width. However, there is a Doppler dependent variation (known as scalloping) which is indicated by the different curves showing (for each ground range position) the performance at the center and max/min Doppler frequency. The range performance is acceptable but for the extreme far range of the swath; nevertheless it is believed that a pattern optimization can yield the required performance, i.e. the antenna height is sufficient to allow for ambiguity suppression.

The burst mode operation has some advantages. Since only part of the swath is illuminated for each burst, the power density can be increased taking advantage of the high gain Tx antenna (assuming a Tx/Rx antenna configuration with TRM), this more or less compensates the reduced power density due to the wider illumination in azimuth. For the same reason the PRF can be increased and by this the total antenna length reduced. The ScanSAR mode is suitable for interferometric applications [14]. The disadvantage is somehow the required increase of the covered Doppler bandwidth by a factor of $n_{burst} + 1$, which at the end results in a reduced Rx antenna gain due to the larger azimuth beamwidth. In total, the ScanSAR mode has an acceptable system efficiency.

3.4 Multi-Azimuth Multi-Elevation Two Burst ScanSAR

An alternative technique to cover a wide swath is the two-burst ScanSAR mode. Here multiple sub-swathes are imaged simultaneously taking advantage of DBF on-receive. To fill the gaps occurring due to the transmit instances, a burst mode operation is utilized, for which two PRFs/bursts are sufficient to fill (cf. **Figure 7a**).

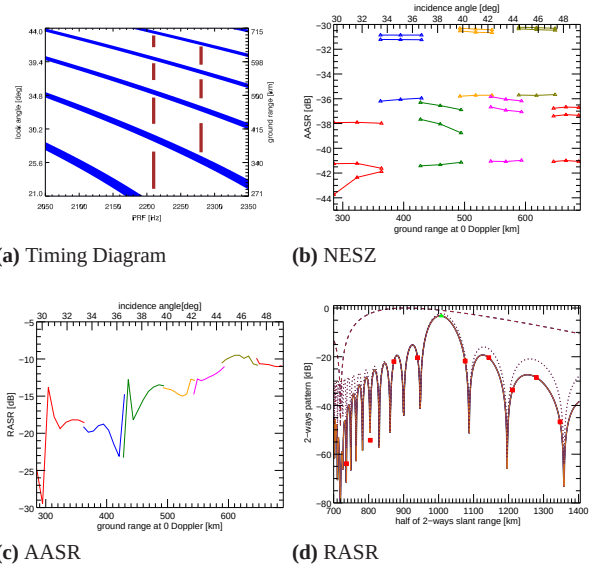

(a) Timing Diagram **(b)** NESZ

(c) AASR **(d)** RASR

Figure 7: Timing diagram and SAR performance of the 2-burst ScanSAR MACs system.

Here the receive antenna dimensions are chosen to be $6.8\,\mathrm{m} \times 5.5\,\mathrm{m}$. This mode gives some flexibility in deciding on the antenna dimensions as long as the minimum antenna area does not go below a critical values. If, for example, the antenna height is increased the range ambiguity suppression will improve allowing an increase in the PRF, which in turn allows to reduce the antenna length. Here, the number of azimuth channels is $N = 3$, which is determined by the length of the antenna element (corresponding to one channel) necessary to cover the system Doppler bandwidth[3].

The azimuth performance, cf. **Figure 7b**, is good, mainly due to the oversampling effect. It is seen that the even numbered sub-swathes have a worse performance; this a result of the different PRF values, which, according to (2) result in an operation at a $3\,\%$ non-uniform azimuth sampling [15]. The elevation performance shown here in terms of the range-ambiguity-to-signal ratio (RASR) does not satisfy the requirement, as seen from **Figure 7c**. Nevertheless, the antenna height of $5.5\,\mathrm{m}$ is considered sufficient for ambiguity suppression if a dedicated beamforming technique is used. From **Figure 7d** it is seen that the angular separation between the pattern nulls are such that they could be positioned at the two nearest ambiguities. Two techniques could be utilized here: suppressing (pattern nulls) the range ambiguities [16], a task which is somehow complicated since the ambiguity suppression strongly depends on the position of the null, and moreover the angular position of ambiguities change from near to far range. Another opportunity is to realize that the ambiguities for one sub-swath are actually signals for the others, which are measured. This is the principal idea of the CEBRAS method [17] of a posteriori removal of the (known) range ambiguities.

The advantage of this mode is that it needs only two bursts. On the other hand there are two main disadvantages which reduce the system efficiency. One is that the number of channels is higher than what is needed to reconstruct the instantaneous Doppler bandwidth, which effectively increases the data rate. The second disadvantage is that the transmit beam illuminates the complete swath, although only part of it (approximately the half) is imaged for each burst; this increases the required power.

4 Parameter Trade Example

One example parameter trade map is shown in **Figure 8** and is explained in the following starting from lower left. The limiting factor for the swath is a timing issue constraint by the available echo window length. Multi-SCORE technique can be used to increase the swath width; here multiple digital beams are generated, each tracking the ground echo of –otherwise– ambiguous signals. However, the total wide swath will contain gaps. To overcome this, the pulse-to-pulse interval is varied over time [3], a technique known as staggered PRF. This

[3]The system Doppler bandwidth corresponds the azimuth beamwidth illuminated by the transmit antenna, whereas the reconstructed Doppler bandwidth, which is smaller than the system bandwidth, yields the azimuth resolution.

displaces the blind ranges across the swath over azimuth time and can be designed to yield a gap-free wide swath. However, it can be shown that this technique increases the side-lobe level of the impulse response function (IRF) of the system, unless the average PRF is increased (approximately doubled) [18]. The system now operates in the somehow unusual mode, where a wide swath is covered despite the high PRF.
The effect of increasing the PRF is twofold. First it results in a higher range ambiguity level; this can at least partly be compensated by applying interference suppression techniques, i.e. elevation DBF. Second, the high PRF basically means an oversampling of the azimuth Doppler spectrum, causing an increase in the data rate. This could be reduced by applying presuming techniques, which, due to the non-uniform azimuth sampling, means data resampling [18]. As a consequence the instrument design requires suitable on-board processing capabilities.

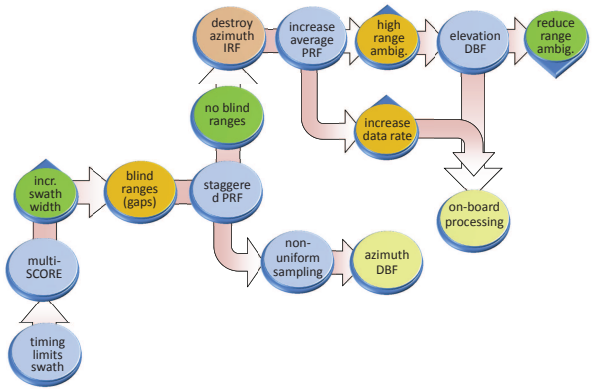

Figure 8: Parameter and techniques trade map for the exemplary MIMO SAR system.

Staggered PRF causes other particularities in the azimuth sampling: it becomes non-uniform and moreover the (intended) changing position of the range gap causes an azimuth sampling behaviour which is range variant. For the case of a single azimuth channel system (low azimuth resolution) interpolation can be utilized [18] from a uniform azimuth grid. However, if a high azimuth resolution is required, the Multiple Azimuth Channels (MACs) technique is required. However, the common reconstruction techniques associated to MACs [15, 12] are not suitable for the case of staggered SAR. Here, new innovative methods, such as for example in [19], are required.

5 Conclusion

The paper presented various techniques suitable for multi-channel SAR systems. The SAR performance of these modes were shown for an exemplary L-band SAR required to image a 400 km swath. The main purpose was to show how the MIMO-SAR trade-space parameters can be utilized and to explain their impact on the system design. Finally a trade map for a staggered MIMO SAR system was given.

References

[1] N. Gebert, "Multi-channel azimuth processing for high-resolution wide-swath sar imaging," Ph.D. dissertation, German Aerospace Center (DLR), Aug. 2009.

[2] M. Younis, "Digital beam-forming for high resolution wide swath real and synthetic aperture radar," Ph.D. dissertation, Institut für Höchstfrequenztechnik und Elektronik, Universität Karlsruhe, July 2004.

[3] G. Krieger, N. Gebert, and A. Moreira, "Multidimensional waveform encoding: A new digital beamforming technique for synthetic aperture radar remote sensing," *IEEE Transactions on Geoscience and Remote Sensing*, vol. 46, no. 1, pp. 31–46, Jan. 2008.

[4] C. Fischer, C. Schaefer, and C. Heer, "Technology development for the HRWS (High Resolution Wide Swath) SAR," in *International Radar Symposium IRS'07*, Sept. 2007.

[5] G. D. Callaghan, "Wide-swath space-borne SAR: Overcoming the trade-off between swath-width and resolution," Ph.D. dissertation, University of Queensland's, 1999.

[6] M. Süß and W. Wiesbeck, "Side-looking synthetic aperture radar system," European Patent EP 1 241 487, Sept., 2002.

[7] M. Younis, T. Rommel, F. Bordoni, G. Krieger, and A. Moreira, "On the pulse extension loss in digital beamforming SAR," *IEEE Geoscience and Remote Sensing Letters*, vol. 12, no. 7, pp. 1436–1440, July 2015.

[8] M. Younis, P. López-Dekker, G. Krieger, and A. Moreira, "Digital beamforming signal-to-noise ratio gain in multi-channel SAR," in *Proc. Int. Geoscience and Remote Sensing Symposium IGARSS'15*, Milan, Italy, July 2015.

[9] M. Younis, P. López-Dekker, F. Bordoni, P. Laskowski, and G. Krieger, "Exploring the trade-space of MIMO SAR," in *Proc. Int. Geoscience and Remote Sensing Symposium IGARSS'13*, Melbourne, Australia, July 2013.

[10] P. López-Dekker, M. Younis, J. A. García, T. Börner, and G. Krieger, "Advanced digital beamforming architectures and operation modes for an enhanced SIGNAL mission concepts," in *Proc. 1st workshop on Ka-band Earth Observation Radar Missions (KEO'12)*, Noordwijk, The Netherlands, Nov. 2012.

[11] M. Younis, P. López-Dekker, A. Patyuchenko, and G. Krieger, "Digital beamforming architecture and techniques for a spaceborne interferometric ka-band

mission," in *Proceedings of the IEEE Radar Conference*, Ottawa, Canada, Apr. 2013.

[12] N. Gebert, G. Krieger, and A. Moreira, "Multichannel ScanSAR for high-resolution ultra-wide-swath imaging," in *Proc. European Conference on Synthetic Aperture Radar EUSAR'08*, Friedrichshafen, Germany, June 2008.

[13] "Integrated tile demonstrator," ESA, Phase 1 Final Report, ESA contract no. 4000103316, 2013.

[14] P. Prats-Iraola, N. Yague-Martinez, S. Wollstadt, T. Kraus, and R. Scheiber, "Demonstration of the applicability of 2-look burst modes in non-stationary scenarios with TerraSAR-X," in *Proc. European Conference on Synthetic Aperture Radar EUSAR'2016*, Hamburg, Germany, June 2016.

[15] G. Krieger, N. Gebert, and A. Moreira, "Unambiguous SAR signal reconstruction from non-uniform displaced phase centre sampling," *IEEE Geoscience and Remote Sensing Letters*, vol. 1, no. 4, pp. 260–264, Oct. 2004.

[16] S. Huber, M. Younis, G. Krieger, A. Patyuchenko, and A. Moreira, "Spaceborne reflector SAR systems with digital beamforming," *IEEE Transactions on Aerospace and Electronic Systems*, vol. 48, no. 4, pp. 3473–3493, Oct. 2012.

[17] G. Krieger, S. Huber, M. Villano, M. Younis, T. Rommel, P. López-Dekker, F. Q. de Almeida, and A. Moreira, "CEBRAS: Cross elevation beam range ambiguity suppression for high-resolution wide-swath and MIMO-SAR imaging," in *Proc. Int. Geoscience and Remote Sensing Symposium IGARSS'15*, Milan, Italy, July 2015, pp. 196–199.

[18] M. Villano, G. Krieger, and A. Moreira, "Staggered SAR: High-resolution wide-swath imaging by continuous PRI variation," *IEEE Transactions on Geoscience and Remote Sensing*, vol. 52, no. 7, pp. 4462–4479, July 2014.

[19] F. Q. de Almeida and G. Krieger, "Multichannel staggered SAR azimuth sample regularization," in *Proc. European Conference on Synthetic Aperture Radar EUSAR'2016*, Hamburg, Germany, June 2016.